



Alkali Lignin and Alkali Combined Ozone-Treated Lignin for Sustainable Food Packaging Applications

Sürdürülebilir Gıda Ambalajlama Uygulamaları için Alkali Lignin ve Ozonla İşlem Görmüş Alkali Lignin Kullanımı

Ece Söğüt[✉] and Atif Can Seydim[✉]

Department of Food Engineering, Faculty of Engineering, Süleyman Demirel University, Isparta, Turkey.

ABSTRACT

This study aimed to utilize the lignin-based structures extracted from chestnut shells, an agricultural waste, in chitosan (CH) films. Lignin (L) was isolated from chestnut shells by alkali treatment (8% NaOH, 120°C/15 min), then sulfuric acid precipitation (0.5M) and drying. In addition, black liquor was treated with ozone to obtain more homogeneous and compatible lignin fractions. Black liquor obtained after an alkali treatment was further treated with ozone at ambient conditions to gain alkali combined ozone-treated lignin (OL). L and OL were added to CH film-forming solutions to fabricate CH-L and CH-OL films and films were characterized by barrier against water (WVP), morphological, thermal properties, optical and antioxidant properties. Fourier transform infrared (FTIR) data confirmed that the isolated L and OL had different structures, and the films indicated a potential interaction between lignin-based structures and CH matrices. Moreover, incorporating L and OL into the CH films increased the opacity and antioxidant activity of films. The addition of lignin-based structures caused a plasticizing effect on the CH films, corresponding with the tensile and thermal properties. The WVP of CH was not significantly influenced upon the addition of lignin-based structures ($p>0.05$).

Key Words

Lignin, Ozonated Lignin, Chitosan, Antioxidant.

Öz

Bu çalışmada, tarımsal bir atık olan kestane kabuğundan elde edilen lignin bazlı yapıların kitosan (CH) filmlerinde kullanılmasını amaçlanmıştır. Lignin (L), alkali uygulaması (%8 NaOH, 120°C/15 dakika) ardından sülfürik asit ile çöktürme (0.5 M) ve kurutma işlemlerinin ardından kestane kabuklarından izole edilmiştir. Bunun yanı sıra, siyah likör daha homojen ve diğer yapılar ile daha uyumlu lignin fraksiyonları elde etmek için ozon ile muamele edilmiştir. Bu amaçla, alkali muamelesinden sonra elde edilen siyah likör, alkali kombine ozon uygulanmış lignin (OL) elde etmek için oda sıcaklığında ozon uygulamasına maruz bırakılmıştır. Elde edilen L ve OL yapıları, CH-L ve CH-OL filmlerini üretmek için CH film çözeltilerine eklenmiş ve elde edilen filmlerin su buharı geçirgenliği (WVP), morfolojik, termal, optik ve antioksidatif özellikleri belirlenmiştir. Fourier transform kızılötesi (FTIR) verileri ile, izole edilmiş L ve OL'nin farklı yapıları sahip olduğu gözlenmiş ve lignin bazlı yapılar ile CH matrisleri arasında potansiyel bir etkileşim olduğu gösterilmiştir. Ayrıca, L ve OL'nin CH filmlerine ilave edilmesi, filmlerin opaklığını ve antioksidan aktivitesini arttırmıştır. Lignin bazlı yapıların CH filmlere eklenmesi, mekanik ve termal özelliklerde gözlenen iyileştirme ile aynı şekilde CH filmler üzerinde plastikleştirici bir etkiye neden olmuştur. Ancak, lignin bazlı yapıların ilave edilmesi, CH filmlerin WVP değerlerini önemli ölçüde etkilememiştir ($p>0.05$).

Anahtar Kelimeler

Lignin, Ozonlanmış Lignin, Kitosan, Antioksidan

Article History: Received: Dec 13, 2021; Revised: Mar 10, 2022; Accepted: Mar 10, 2022; Available Online: Jul 5, 2022.

DOI: <https://doi.org/10.15671/hjbc.1033151>

Correspondence to: E. Söğüt, Department of Food Engineering, Süleyman Demirel University, Isparta, Turkey.

E-Mail: eccecad@sd.u.edu.tr

INTRODUCTION

Currently, petroleum-based synthetic polymers, non-biodegradable materials, have been extensively used as packaging materials as they have good thermomechanical properties, and they are cost-effective with being lightweight. However, these polymeric materials cause several problems such as global warming, depletion of non-renewable sources, increasing energy demand, increasing food and water shortage, and destruction of rainforests [1]. Therefore, environmentally friendly materials obtained from renewable sources have been extensively studied to replace petroleum-based materials.

The materials from renewable sources can be used to develop new sustainable packaging materials [2]. Chitosan (CH), which is obtained from crustacean shells or insects by N-deacetylation, has antimicrobial effects due to its cationic groups creating electrostatic interactions with anionic groups of cell walls of various microorganisms [3, 4]. The intrinsic antimicrobial activity of CH can be used to prepare active packaging materials. However, due to its poor mechanical resistance and high affinity to water, it is used in limited applications [5, 6].

Recently, lignocellulosic fibers obtained from agro-industrial wastes have been extensively studied to utilize them as sustainable products, potentially reducing the dependence on petroleum-based materials [7]. The landfilling of agro-industrial wastes and further incineration of them result in additional environmental threats; thus, their utilization provides an environmentally friendly solution due to the partial degradation. The lignocellulosic structures (lignin, hemicellulose, and cellulose) are extracted from various parts including stalk, stem, seed, leaf, grass/reed, and fruit of agricultural wastes [8]. The nut shells such as chestnut shells are generally converted into fuel as solid (coal), liquid (ethanol, biodiesel, etc.) and gas (biogas, etc.) by using it as biomass [9]. In recent years, intensive research has been carried out on alternative application areas for the utilization of these components, such as using the lignin in these shells as value-added materials. These waste materials can be utilized as films or coatings with antimicrobial and antioxidant properties or as fillers in polymeric structures while reducing the carbon footprints arising from their burning [2]. Thus, one of those nut shells, chestnut shells, was selected as lignocellulose source to be used in CH films.

Lignin (L) is an amorphous phenolic polymer with a complex structure produced by the copolymerization of three phenylpropanoid monomers [8]. L also has antimicrobial, antioxidant, and light barrier properties [8, 10]. Although L has been used as fillers in various polymers [11–14], poor dispersion and compatibility of L in these polymers limit its applications [15]. Therefore, recent studies have focused on the modification of L by different techniques such as alkylation [16], acetylation [17], hydroxy methylation [18], and ozonation [10]. In the ozonation process, ozone attacks aromatic rings of L and activates these fractions positioned at lignin surface [19, 20]. This process produces carboxyl groups, having the potential to increase the solubility of the L and create esterification sites [19, 20]. Then the resultant ozonated L (OL) could be used in further applications.

Two major problems threaten the environment: the over-use of petroleum-based materials and the landfilling of agricultural residues. Therefore, this study aims to solve these problems by utilizing chestnut shell lignin as an additive in CH-based films. Among the active packaging applications, converting an agro-waste into a filler (L) with antioxidant properties in bio-based polymers (CH) has a great potential. Besides, to improve the reactivity of L, an ozonation process was applied. The effectiveness L and OL addition to the properties of CH films including the water barrier, mechanical, thermal, surface, and active properties were determined.

MATERIALS and METHODS

Materials

Chestnuts were purchased by a local producer in Aydın and peeled to collect shells (CS). CS was then dried at 75°C and ground (average particle size of 300 µm) before storing at 4°C until use. Chitosan (CH) (ChitoClear® CG1600, >320 kDa, and more than 75% of deacetylated) was supplied by Primex (Siglufjördur, Iceland). The other chemicals were obtained from Sigma-Aldrich (St. Louis, Missouri, USA) as of analytical grade.

Ozonation and Characterization of Lignin-based Structures

The de-lignification steps of CS are presented in Figure 1. Briefly, CS (a liquid/solid ratio of 10%, w/w) was firstly exposed to water extraction to remove the hemicellulose and water-soluble extracts and then treated with NaOH (8%, w/w) at 121°C for 15 min. The water extraction step before alkali treatment has the potential to increase lignin

yield for lignin degradation processes to be carried out in later stages [21]. Black liquor was collected after filtration and washing until neutral pH was reached. The collected liquor was exposed to H_2SO_4 (to pH 2) for lignin precipitation. The obtained solid phase was dried at $70^\circ C$ after filtration and washing with acid to obtain solid lignin (L). The black liquor was also modified by ozonation for 60 min [10]. Ozone was generated by an ozone generator (Ozotech OZ4PC10, Yreka, CA) with an ozone concentration of 0.65 ppm. After the ozonation process, insoluble parts were removed by filtration, and ozonated lignin structures were collected by precipitating with acidified water at pH 2.0 (H_2SO_4). The solid part was washed and dried at $50^\circ C$ to obtain ozonated lignin (OL).

The properties of L and OL were screened by Fourier transform infrared (FTIR) spectrums, ranging from 500 cm^{-1} to 4000 cm^{-1} (Spectrum Two, Perkin Elmer, USA).

Preparation of Film Samples

CH film-forming solution (1%, w/w) was prepared in an acidic medium (acetic acid, 1%, w/w) followed by the addition of glycerol (0.3%, w/w) as plasticizer. L and OL at 10% (w/w, based on CH) were added to this solution and the solutions were mixed. The air bubbles were removed by vacuum and the adjusted amounts of the film-forming solutions were poured onto Teflon® coated plates with a diameter of 150 mm. The conditioning step was carried out at $25^\circ C$ and 53% relative humidity (RH) for one week after peeling the dried films. CH film was chosen as the control film, and other film samples were named CH-L and CH-OL films, including L and OL, respectively. The thickness of final films was also recorded with a micrometer (Quantu-Mike IP65, Mitutoyo, Japan).

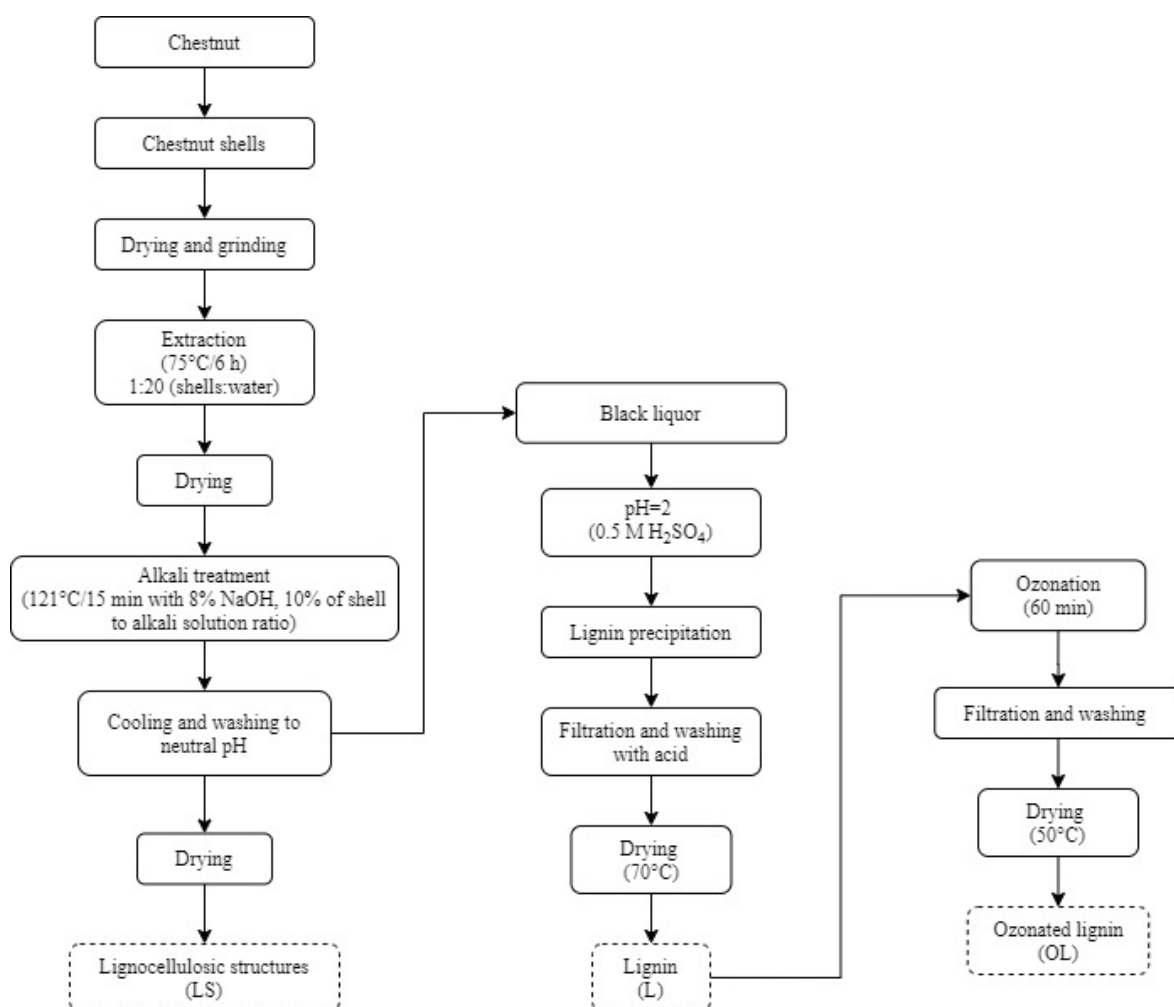


Figure 1. Schematic representation of obtaining L and OL structures .

Characterization of Film Samples

The changes in the film structure were assessed by FTIR spectra ($500\text{--}4000\text{ cm}^{-1}$) recorded with the FTIR spectrometer (Spectrum Two, Perkin Elmer, USA).

The effect of the addition of L and OL on the surface characteristics was assessed using scanning electron microscopy (SEM) (Quanta 450 FEG, Oregon, USA). The microstructural images were obtained at low vacuum medium (10 kV of accelerating voltage).

The mechanical resistance of film samples was calculated with strain-stress curves obtained from the tensile tests (Lloyd LR5, AMETEK, Inc, UK) based on the ASTM D882 reference method [22]. For the experiments, films were mounted with film-extension grips operating at 50 mm/min.

The ASTM E96/E96M-16 [23] based on cup method was used to determine the water vapor permeability (WVP). Films were transferred to permeability cups, including distilled water (5 mL), and the weight changes arising from the differences in relative humidity at each side of films during 48 h were recorded. The transmission rate of water was calculated by linear regression using the slopes obtained after reaching the steady state period for weight loss as a function of time. WVP measurements were performed using the transmission values [24].

The thermal properties of film samples were determined by a thermogravimetric analyzer (Hitachi, NEXTA STA 200, USA) to assess the addition of L and OL how affected the thermal stability. Briefly, 5-8 mg of film sample was weighed and heated at $10^\circ\text{C}/\text{min}$ ($25\text{--}450^\circ\text{C}$) with a nitrogen flux of $20\text{ cm}^3/\text{min}$. The weight loss during the heating was measured using the thermogravimetric (TG) curves.

The opacity of film samples was measured using the absorbance of the film sample ($1\times 4\text{ cm}$ rectangular film strips) at 660 nm (Shimadzu, UV-1601, Japan) and measured by using the related film thickness (absorbance units (AU) $\text{nm}/\mu\text{m}$).

The color measurement was carried out using a colorimeter (CR-400, Konica Minolta, Inc., Japan) as CIE L^* (lightness), a^* (red-green) and b^* (yellow-blue) coordinates. The background was the white standard calibration plate with the values of $Y = 92.7$, $x = 0.3160$, $y = 0.3321$.

The antioxidant capacity of films, L, and OL were evaluated as the inhibition percentage of the DPPH radical. Film

samples were dissolved in an acidic media (acetic acid, 1%, w/w) while L and OL were dissolved in aqueous dioxane (90%, v/v) solution and treated with DPPH radical for 40 min at 25°C . The antioxidant activity was measured using the absorbance of each solution at 517 nm as the inhibition percentage of DPPH radical.

Statistical Analysis

Minitab 17 (Minitab Inc., Brandon, UK) statistical package was used to find the differences among film samples at a 95% confidence level. An analysis of variance (ANOVA) and Tukey's multiple comparison tests were used with three observations for each sample and three replicates.

RESULTS and DISCUSSION

Properties of Extracted Lignin-based Structures

FTIR spectrums of L and OL ozonated during 60 min are presented in Figure 2.

Ozonated lignin structures showed different FTIR spectrums depending on the ozonation period.

The major peaks observed at 1100 cm^{-1} , 1650 cm^{-1} , and $\sim 3300\text{ cm}^{-1}$ were associated with the vibration of ether bonds, the --C=O groups vibrational stretching, and the absorption of free phenolic hydroxyl, as also indicated by Zhang et al. [25]. The ozonation process resulted in changes in the peaks around $1500\text{--}1600\text{ cm}^{-1}$, 800 cm^{-1} , 1000 cm^{-1} , and, 1200 cm^{-1} . Similar changes were also reported by Souza-Corrêa et al. [26] for sugar cane bagasse lignin after the ozonation process. During the ozonation process, lignin is first oxidized to hydroxyl and phenol groups, and further oxidation causes a fraction of benzene to produce more carboxyl and ketone groups [27]. Kwon et al. [28] and Barrera-Martinez et al. [29] reported that the aromatic structures could be selectively attacked by ozone, and the side chains on the benzene ring could be preserved. The intensities of peaks between $1400\text{--}1600\text{ cm}^{-1}$ decreased, which might be related to the breakage of the benzene ring by ozonation [30]. The peaks that appear at $\sim 1700\text{ cm}^{-1}$ related to C=O stretching (ester, ketone, and carboxyl groups) were observed, indicating that ozone might partially degrade aromatic rings and release the carboxyl groups into the lignin matrix. Similarly, Mamleeva et al. [31] observed that ozone treatment destroyed aromatic structures in pine wood.

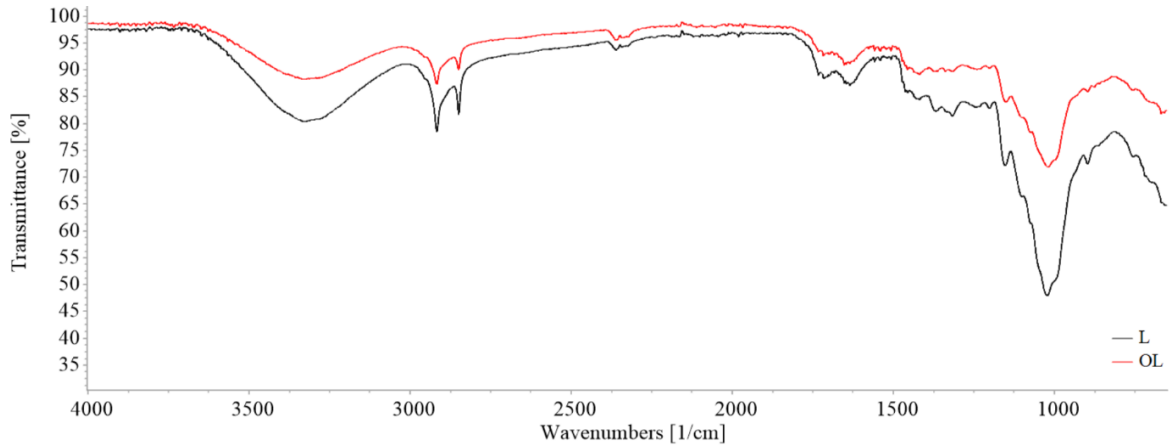


Figure 2. FTIR spectrums of L and OL ozonated during 60 min.

Properties of Film Samples

The physico-mechanical properties including elongation (E), tensile strength (TS), thickness, WVP of films are presented in Table 1.

The TS of film samples enhanced after adding the lignin-based structures ($p < 0.05$). The presence of lignin increased the TS values indicating a good reinforcement. CH-L films had the highest TS values, while CH-OL had the highest elongation ($p < 0.05$). Ozonated lignin incorporati-

on led to an increase in elasticity which might be due to the plasticizing effect. L-based structures have previously been reported to enhance mechanical properties of CH [32, 33], agar [34], and cellulose [35] based films, which might be related to the lignin stability and hydrogen bonds formed within the polymer matrix [36]. Contrary to these results, Crouvisier-Urien et al. [4] and Rai et al. [37] stated that the low compatibility between L and CH decreased the TS and E values.

Table 1. TS, elongation at break, thickness, and WVP values of film samples.

Sample	TS (MPa)	E (%)	Thickness (μm)	WVP (g mm/kPa h m^2)
CH	12.88 \pm 0.16 ^b	19.52 \pm 2.07 ^b	60.7 \pm 14.4 ^b	11.22 \pm 1.89 ^a
CH-L	17.84 \pm 4.07 ^a	19.32 \pm 5.66 ^b	89.5 \pm 16.4 ^a	8.42 \pm 0.98 ^a
CH-OL	14.98 \pm 3.25 ^{ab}	26.75 \pm 3.16 ^a	70.5 \pm 8.3 ^b	9.47 \pm 1.30 ^a

^{a,b} Different superscripts in the same column are significantly different ($p < 0.05$) according to Tukey's test.

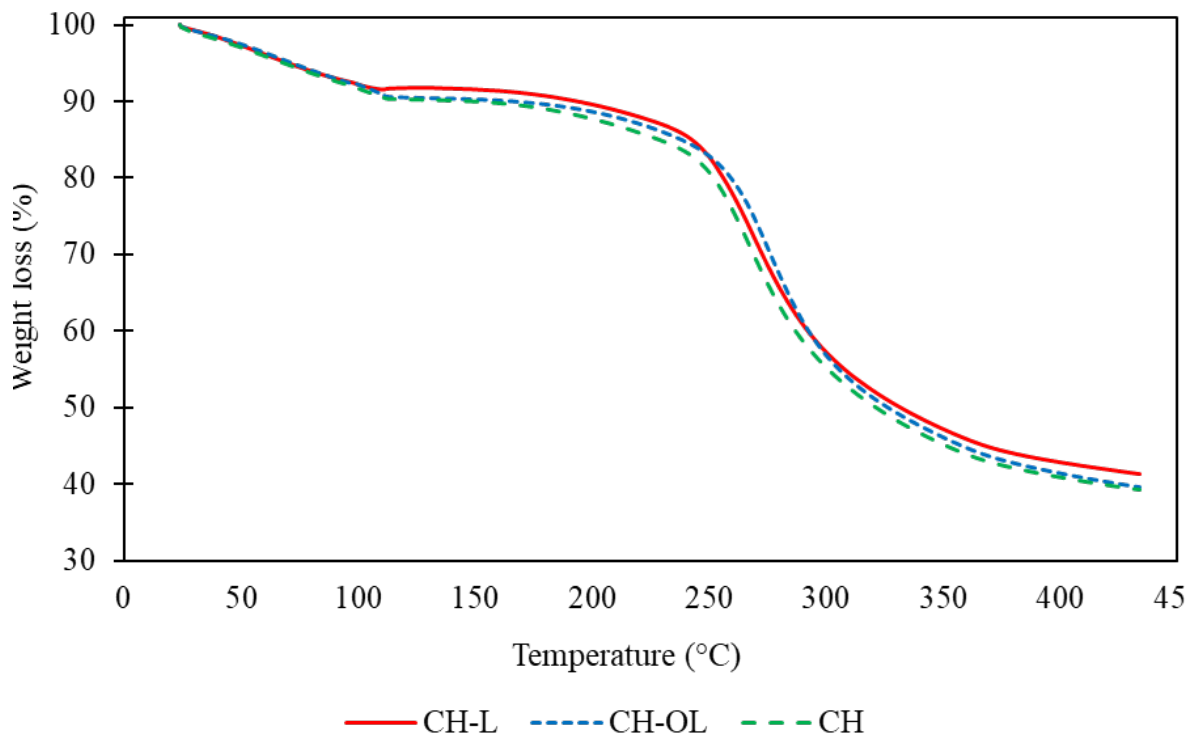


Figure 3. Thermal degradation curves of film samples.

The incorporation of lignin-based structures slightly increased the thickness ($p < 0.05$). Similarly, Rai et al. [37] reported higher thickness values for lignin added CH films depending on the lignin concentration. The addition of L-based structures did not significantly decrease the WVP values of CH films. OL added films had slightly higher WVP values compared to CH-L ($p > 0.05$). The lower WVP values obtained for CH films including lignin might be related to the water repellent properties of aromatic moieties naturally found in lignin structure [37]. The slightly higher WVP values found in CH-OL compared to CH-L films could be related to the compatibility of L with CH and OL with CH. A similar reducing effect of L-based structures was observed by Yang et al. [38] and Shankar and Rhim [34] for poly(lactic acid) and agar-based films, respectively. The insoluble nature of L could obtain lower WVP values by increasing the hydrophobic character of films, as also stated by Aadil et al. [11].

The thermal degradation behavior of film samples is presented in Figure 3.

Film samples presented a similar trend during the thermal analysis, which experienced an initial weight loss at approximately 120 °C followed by a second weight loss between 190 and 350 °C. The weight loss observed at 120 °C was due to the evaporation of water found in film samples. The degradation of the acetylated and deacetylated units of CH and L-based structures caused the second weight loss observed between 190 and 350 °C. Besides, the degradation temperature of CH films reached a bit higher degree after the addition of L-based structures, indicating that L and OL could stabilize the degradation of CH films, to an extent. Lignin could create a more complex structures (aromatic structure) at high temperatures leading to decrease the extent of decomposition in the film structure [39]. Besides, Chen et al. [40], Nair et al. [41], and Aradmehr and Javanbakh [39] reported similar thermal properties for CH films when incorporated with L-based structures.

The optical properties of film samples are presented in Table 2.

Table 2. Optical properties of film samples.

Sample	Opacity (AU nm/ μ m)	L*	a*	b*
CH	1.69 \pm 0.54 ^b	94.98 \pm 0.12 ^a	-0.01 \pm 0.03 ^c	6.19 \pm 0.38 ^c
CH-L	3.62 \pm 0.49 ^a	74.32 \pm 2.03 ^c	3.94 \pm 0.37 ^a	15.74 \pm 1.12 ^a
CH-OL	2.35 \pm 0.15 ^{ab}	86.23 \pm 0.62 ^b	1.27 \pm 0.10 ^b	12.45 \pm 0.63 ^b

^{a,b} Different superscripts in the same column are significantly different ($p < 0.05$) according to Tukey's test.

The incorporation of L led to higher opacity values while lowering the lightness values ($p < 0.05$). L and OL incorporated film samples presented significantly higher opacity, indicating that these films might be an efficient light barrier. Besides, CH films had the highest lightness values, whereas the significantly higher a^* and b^* values for L and OL added CH films were observed ($p < 0.05$), as can be seen in Figure 4.

Sa et al. [33] also observed increased opacity with improved UV-barrier properties for CH films when incorporated with cellulose-lignin-cellulose nanocrystal from cashew byproducts. L naturally had a dark brown color, while a lighter brown color was obtained after the ozonation. Thus, OL provided the CH films with less color and lightness change than L did, which might be due to the chromophore nature of lignin [42]. Similar changes in the color of CH films with the incorporation of L, organosolv treated L, and fractionated L-based structures by Izaguirre et al. [32].

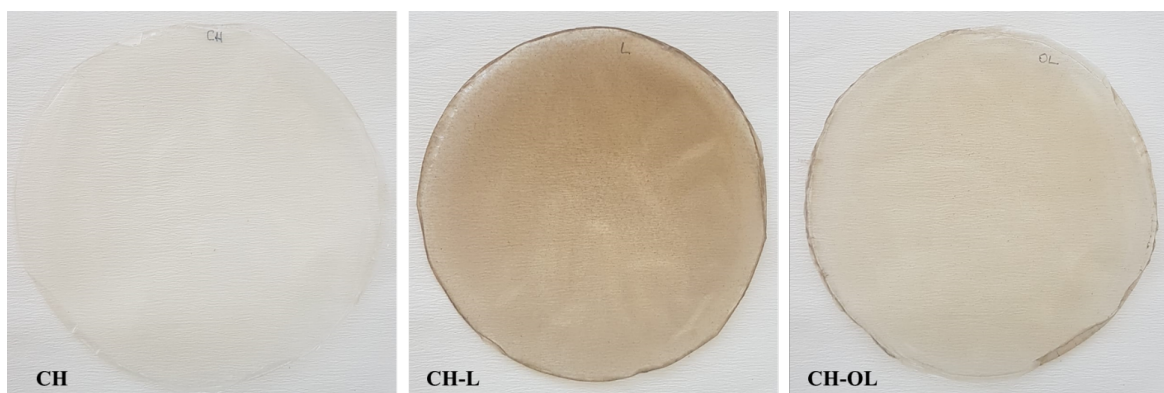


Figure 4. Images of film samples (CH: control films, CH-L: CH films with lignin, CH-OL: CH films with ozonated lignin).

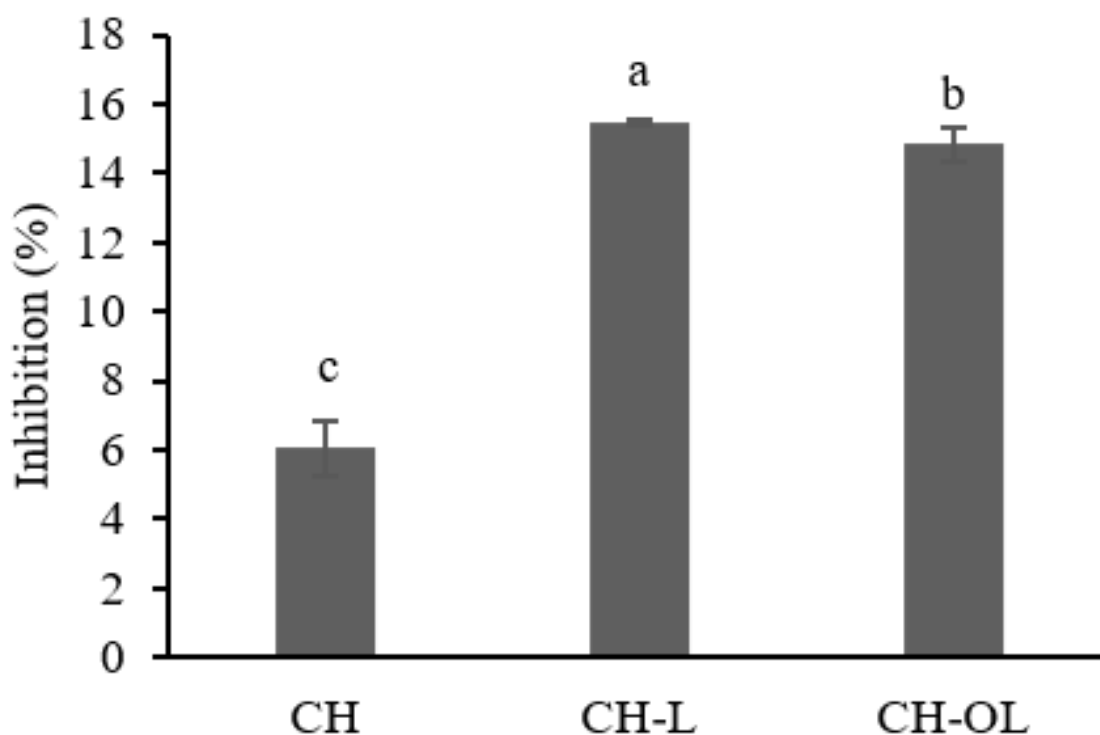


Figure 5. Antioxidant activity of film samples. a-c Different letters are significantly different ($p < 0.05$).

The potential antioxidant capacities of CH films, including L-based structures, were examined using the DPPH• radical scavenging ability of films to assess whether L-based structures maintained their ability within the polymeric matrix. L and OL showed 44.72 ± 3.93 and $35.39 \pm 1.08\%$ DPPH scavenging activity, respectively (Figure 5). CH films already had natural antioxidant activity without the addition of L-based structures. The amino and hydroxyl groups found in CH were the reason for CH films' antioxidant activity [43]. Besides, notable increases were observed in antioxidant activities with the addition of L and OL. The antioxidant activity brought by L might be related to the high free phenolic hydroxyl groups, their migration from the film matrix and surface activity, and [39]. This behavior was already observed by Crouvisier-Urien et al. [4], Crouvisier-Urien et al. [44], and Aradmehr and Javanbakh [39] for CH films in which lignin addition induced higher antioxidant activity values as a function of lignin concentration. The lower antioxidant activity obtained for CH-OL than CH-L could be related to the oxidation of some phenolic residues during the ozonation process, thus decreasing the activity [10].

FTIR spectrums of film samples were obtained to reveal whether an interaction was established between CH and L-based structures (Figure 6).

The major peaks observed in FTIR spectrums were at $3100\text{--}3500\text{ cm}^{-1}$ ascribed to hydroxyl groups, at $3400\text{--}3300\text{ cm}^{-1}$ related to amino groups, at $\sim 3280\text{ cm}^{-1}$ associated with the vibrations of NH groups, at $1650\text{--}1550\text{ cm}^{-1}$ for Amide I-II bands, and 1500 cm^{-1} assigned to non-protonated amino groups of CH [45]. The observed bands for CH-L and CH-OL films were similar to the characteristic bands of CH-based films without any reinforcement. The peak at 3300 cm^{-1} for OH groups slightly shifted in CH-L, and CH-OL films and minor changes were detected between $1600\text{--}1670\text{ cm}^{-1}$ assigned for amide bonds and stretching vibrations of C-O. The changes found in peak intensities and band shifts might be related to the possible interactions between OH, =CO (in CH films) and ether groups (in L-based structures) via hydrogen bonding [37]. Even though the intensities of peaks $1600\text{ cm}^{-1} - 1450\text{ cm}^{-1}$ decreased due to the cleavage of benzene rings by ozonation, there is still aromatic ring vibrations between these absorption range, sugges-

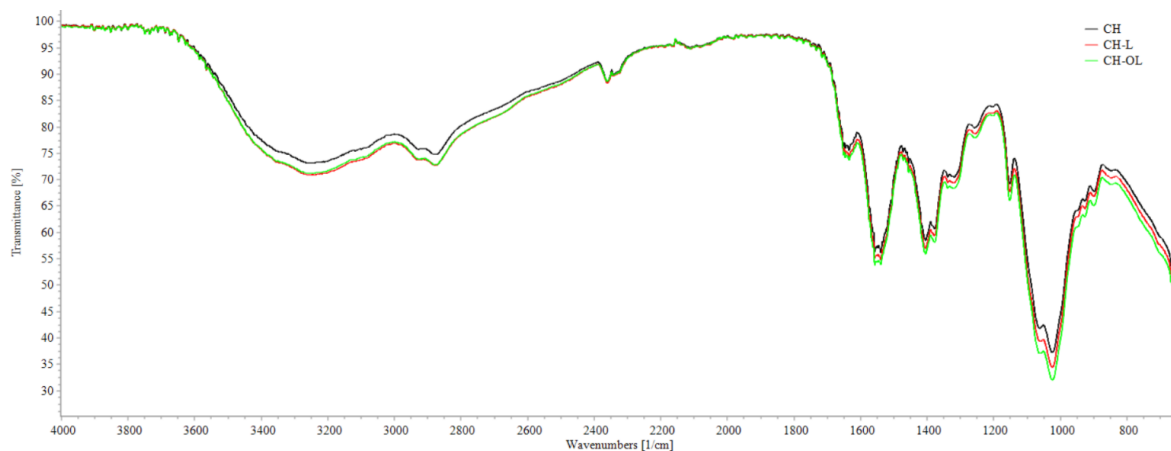


Figure 6. FTIR spectrums of film samples.

ting that the ozonation could not completely destroy the benzene ring. Besides, after the ozonation, the partially degradation of aromatic rings and the release of carboxyl groups into the matrix might contribute to those obtained interactions. Similar FTIR spectrums were observed by Rosova et al. [46], Aradmehr and Javanbakh [39], and Chen et al. [40] for CH films, including L-based structures.

The surface morphology images of films are presented in Figure 7.

CH films showed smooth and homogeneous structure, whereas incorporating L and OL in the CH films resulted in more heterogeneous surfaces. L increased the roughness of CH film with noticeable lignin aggregates at the film surface, and OL presented a more homogeneous microstructure than CH-L films. Similarly, Crouvisier-Urien et al. [4] and Sa et al. [33] stated increased surface roughness of CH films incorporated with lignin. The improvement in tensile and water barrier properties observed in CH-L and CH-OL films, even having rough surfaces, might be associated with the modification on the film surface composition.

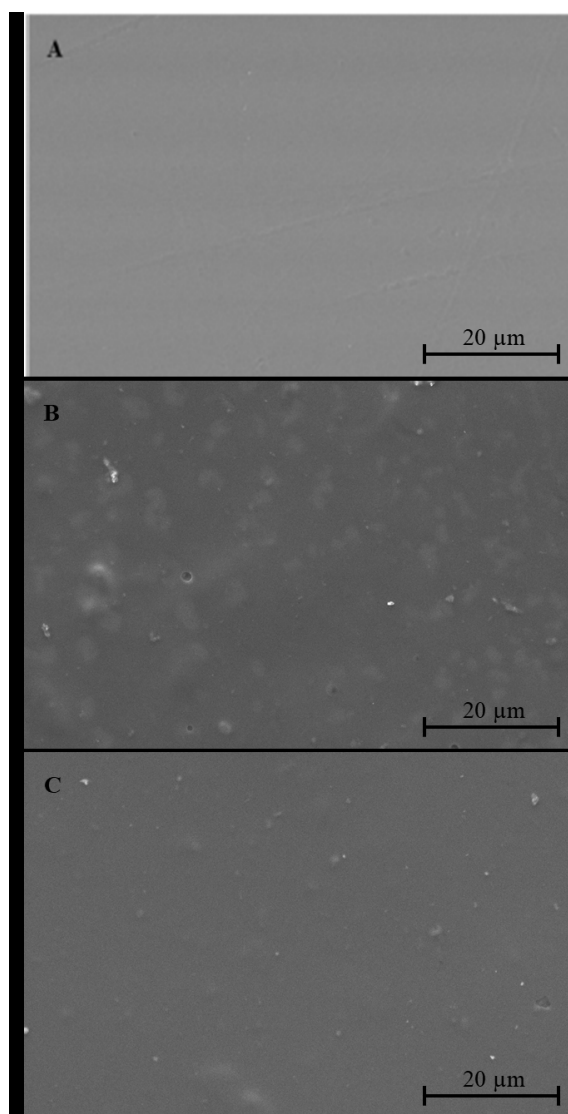


Figure 7. SEM images of film samples (A=CH, B=CH-L, C=CH-OL) (3000X magnification for all film samples).

CONCLUSION

Lignin obtained from agricultural wastes could improve the properties of packaging materials and provide a contribution to the re-design of sustainable packaging materials having active properties. Therefore, in this study, chestnut shells, one of the agro-wastes, were de-lignified under an alkaline medium to obtain lignin (L), and the resultant structure was ozonated (OL) for incorporation in chitosan (CH) film. The water barrier and the mechanical strength of films incorporated lignin-based structures increased; however, the addition of fillers based on agro-waste reduced the lightness values of CH films. Film samples showed similar thermal degradation behavior and FTIR spectrums compared to control films. According to the SEM images, CH films had a smooth surface, and OL added CH films presented better surface properties than CH-L films. Film samples incorporated with L had higher values ($p < 0.05$) according to the DPPH radical scavenging activity test. These results presented that adding lignin into biopolymeric films could produce enhancement in biopolymers while providing functional properties including antioxidant activity.

References

1. Michelin M., Marques A.M., Pastrana L.M., Teixeira J.A., Cerqueira M.A., Carboxymethyl cellulose-based films: Effect of organosolv lignin incorporation on physicochemical and antioxidant properties, *J. Food Eng.*, 2020, 285, 110107.
2. Ballesteros L.F., Michelin M., Vicente A.A., Teixeira J.A., Cerqueira M.Á., Food Applications of Lignocellulosic-Based Packaging Materials, 2018, 87–94.
3. Kong M., Chen X.G., Xing K., Park H.J., Antimicrobial properties of chitosan and mode of action: A state of the art review, *Int. J. Food Microbiol.*, 2010, 144, 51–63.
4. Crouvisier-Urien K., Bodart P.R., Winckler P., Raya J., Gougeon R.D., Cayot P., *et al.*, Biobased composite films from chitosan and lignin: antioxidant activity related to structure and moisture, *ACS Sustain. Chem. Eng.*, 2016, 4, 6371–6381.
5. Sogut E., Seydim A.C., Development of Chitosan and Polycaprolactone based active bilayer films enhanced with nanocellulose and grape seed extract, *Carbohydr. Polym.*, 2018, 195, 180–188.
6. Söğüt E., Seydim A.C., Characterization of cyclic olefin copolymer-coated chitosan bilayer films containing nanocellulose and grape seed extract, *Packag. Technol. Sci.*, 2018, 31, 499–508.
7. Sogut E., Cakmak H., Utilization of carrot (*daucus carota* L.) Fiber as a filler for chitosan based films, *Food Hydrocoll.*, 2020, 105861.
8. Saini J.K., Saini R., Tewari L., Lignocellulosic agriculture wastes as biomass feedstocks for second-generation bioethanol production: concepts and recent developments, *3 Biotech*, 2015, 5, 337–353.
9. Guney M.S., Utilization of hazelnut husk as biomass, *Sustain. Energy Technol. Assessments*, 2013, 4, 72–77.
10. Shi C., Zhang S., Wang W., Linhardt R.J., Ragauskas A.J., Preparation of Highly Reactive Lignin by Ozone Oxidation: Application as Surfactants with Antioxidant and Anti-UV Properties, *ACS Sustain. Chem. Eng.*, 2020, 8, 22–28.
11. Aadil K.R., Prajapati D., Jha H., Improvement of physicochemical and functional properties of alginate film by Acacia lignin, *Food Packag. Shelf Life*, 2016, 10, 25–33.
12. Gordobil O., Egüés I., Llano-Ponte R., Labidi J., Physicochemical properties of PLA lignin blends, *Polym. Degrad. Stab.*, 2014, 108, 330–338.
13. Miao C., Hamad W.Y., Controlling lignin particle size for polymer blend applications, *J. Appl. Polym. Sci.*, 2017, 134
14. Sahoo S., Misra M., Mohanty A.K., Biocomposites from switchgrass and lignin hybrid and poly (butylene succinate) bioplastic: Studies on reactive compatibilization and performance evaluation, *Macromol. Mater. Eng.*, 2014, 299, 178–189.
15. Kazzaz A.E., Feizi Z.H., Fatehi P., Grafting strategies for hydroxy groups of lignin for producing materials, *Green Chem.*, 2019, 21, 5714–5752.
16. Zhang T., Zhou Y., Liu D., Petrus L., Qualitative analysis of products formed during the acid catalyzed liquefaction of bagasse in ethylene glycol, *Bioresour. Technol.*, 2007, 98, 1454–1459.
17. Rowell R.M., Dickerson J.P., Acetylation of wood, In: *Deterioration and Protection of Sustainable Biomaterials*, ACS Publications, 2014, 301–327.
18. Mohamad Aini N.A., Othman N., Hussin M.H., Sahakaro K., Hayeemasae N., Hydroxymethylation-modified lignin and its effectiveness as a filler in rubber composites, *Processes*, 2019, 7, 315.
19. Ma R., Xu Y., Zhang X., Catalytic oxidation of biorefinery lignin to value-added chemicals to support sustainable biofuel production, *ChemSusChem*, 2015, 8, 24–51.
20. Schutyser W., Renders T., Van Den Bosch S., Koelewijn S.F., Beckham G.T., Sels B.F., Chemicals from lignin: An interplay of lignocellulose fractionation, depolymerisation, and upgrading, *Chem. Soc. Rev.*, 2018, 47, 852–908.
21. Ingram T., Wörmeyer K., Lima J.C.I., Bockemühl V., Antranikian G., Brunner G., *et al.*, Comparison of different pretreatment methods for lignocellulosic materials. Part I: Conversion of rye straw to valuable products, *Bioresour. Technol.*, 2011, 102, 5221–5228.
22. American Society for Testing and Materials, Standard Test Method for Tensile Properties of Thin Plastic Sheeting, ASTM International, www.Astm.Org, 2018.
23. American Society for Testing and Materials Standard, Standard test methods for water vapor transmission of materials: E96/E96M- 16. Annual book of American society for testing and materials standards, *Annu. B. Am. Stand. Test. Methods*, 2016, 04.06, 14.
24. Villalobos R., Hernández-Muñoz P., Chiralt A., Effect of surfactants on water sorption and barrier properties of hydroxypropyl methylcellulose films, *Food Hydrocoll.*, 2006, 20, 502–509.
25. Zhang Y., Yan R., Ngo T. dung, Zhao Q., Duan J., Du X., *et al.*, Ozone oxidized lignin-based polyurethane with improved properties, *Eur. Polym. J.*, 2019, 117, 114–122.
26. Souza-Correia J.A., Ridenti M.A., Oliveira C., Araújo S.R., Amorim J., Decomposition of lignin from sugar cane bagasse during ozonation process monitored by optical and mass spectrometries, *J. Phys. Chem. B*, 2013, 117, 3110–3119.
27. Schultz-Jensen N., Leipold F., Bindsløv H., Thomsen A.B., Plasma-assisted pretreatment of wheat straw, *Appl. Biochem. Biotechnol.*, 2011, 163, 558–572.

28. Kwon J.Y., Chung P.G., Lim I.H., Removal of residual COD in biologically treated paper-mill effluent and degradation of lignin using nonthermal plasma unit, *J. Environ. Sci. Heal. - Part A Toxic/Hazardous Subst. Environ. Eng.*, 2004, 39, 1853–1865.
29. Barrera-Martínez I., Guzmán N., Peña E., Vázquez T., Cerón-Camacho R., Folch J., *et al.*, Ozonolysis of alkaline lignin and sugarcane bagasse: Structural changes and their effect on saccharification, *Biomass and Bioenergy*, 2016, 94, 167–172.
30. Du X., Wu S., Li T., Yin Y., Zhou J., Ozone oxidation pretreatment of softwood kraft lignin: An effective and environmentally friendly approach to enhance fast pyrolysis product selectivity, *Fuel Process. Technol.*, 2022, 231, 107232.
31. Mamleeva N.A., Babayeva N.A., Kharlanov A.N., Lunin V. V., Destruction of Lignin during the Ozonation of Pine Wood, *Russ. J. Phys. Chem. A*, 2019, 93, 28–33.
32. Izaguirre N., Gordobil O., Robles E., Labidi J., Enhancement of UV absorbance and mechanical properties of chitosan films by the incorporation of solvolytically fractionated lignins, *Int. J. Biol. Macromol.*, 2020, 155, 447–455.
33. Sá N.M.S.M., Mattos A.L.A., Silva L.M.A., Brito E.S., Rosa M.F., Azeredo H.M.C., From cashew byproducts to biodegradable active materials: Bacterial cellulose-lignin-cellulose nanocrystal nanocomposite films, *Int. J. Biol. Macromol.*, 2020, 161, 1337–1345.
34. Shankar S., Rhim J.W., Preparation and characterization of agar/lignin/silver nanoparticles composite films with ultraviolet light barrier and antibacterial properties, *Food Hydrocoll.*, 2017, 71, 76–84.
35. Chen Y., Fan D., Han Y., Lyu S., Lu Y., Li G., *et al.*, Effect of high residual lignin on the properties of cellulose nanofibrils/films, *Cellulose*, 2018, 25, 6421–6431.
36. Yang W., Fortunati E., Dominici F., Giovanale G., Mazzaglia A., Balestra G.M., *et al.*, Effect of cellulose and lignin on disintegration, antimicrobial and antioxidant properties of PLA active films, *Int. J. Biol. Macromol.*, 2016, 89, 360–368.
37. Rai S., Dutta P.K., Mehrotra G.K., Lignin incorporated antimicrobial chitosan film for food packaging application, *J. Polym. Mater.*, 2017, 34, 171–183.
38. Yang W., Weng Y., Puglia D., Qi G., Dong W., Kenny J.M., *et al.*, Poly(lactic acid)/lignin films with enhanced toughness and anti-oxidation performance for active food packaging, *Int. J. Biol. Macromol.*, 2020, 144, 102–110.
39. Aradmehr A., Javanbakht V., A novel biofilm based on lignocellulosic compounds and chitosan modified with silver nanoparticles with multifunctional properties: Synthesis and characterization, *Colloids Surfaces A Physicochem. Eng. Asp.*, 2020, 600, 124952.
40. Chen L., Tang C., Ning N., Wang C., Fu Q., Zhang Q., Preparation and properties of chitosan/lignin composite films, *Chinese J. Polym. Sci.*, 2009, 27, 739–746.
41. Nair V., Panigrahy A., Vinu R., Development of novel chitosan-lignin composites for adsorption of dyes and metal ions from wastewater, *Chem. Eng. J.*, 2014, 254, 491–502.
42. Shankar S., Reddy J.P., Rhim J.W., Effect of lignin on water vapor barrier, mechanical, and structural properties of agar/lignin composite films, *Int. J. Biol. Macromol.*, 2015, 81, 267–273.
43. Xie W., Xu P., Liu Q., Antioxidant activity of water-soluble chitosan derivatives, *Bioorganic Med. Chem. Lett.*, 2001, 11, 1699–1701.
44. Crouvisier-Urien K., Lagorce-Tachon A., Lauquin C., Winckler P., Tongdeesoontorn W., Domenek S., *et al.*, Impact of the homogenization process on the structure and antioxidant properties of chitosan-lignin composite films, *Food Chem.*, 2017, 236, 120–126.
45. Van De Velde K., Kiekens P., Structure analysis and degree of substitution of chitin, chitosan and dibutyrilchitin by FT-IR spectroscopy and solid state¹³C NMR, *Carbohydr. Polym.*, 2004, 58, 409–416.
46. Rosova E., Smirnova N., Dresvyanina E., Smirnova V., Vlasova E., Ivan'kova E., *et al.*, Biocomposite materials based on chitosan and lignin: Preparation and characterization, *Cosmetics*, 2021, 8, 1–17.